



Crystal Chemistry of Three Volcanic K-rich Nepheline Samples From Oldoinyo Lengai, Tanzania and Mount Nyiragongo, Eastern Congo, Africa

Sytle M. Antao* and James W. Nicholls

Department of Geoscience, University of Calgary, Calgary, AB, Canada

OPEN ACCESS

Edited by:

Fabrice Brunet,
UMR5275 Institut des Sciences de la
Terre (ISTERRE), France

Reviewed by:

Anthony Martin Thomas Bell,
Sheffield Hallam University,
United Kingdom

Martin Charles Wilding,
Sheffield Hallam University,
United Kingdom

*Correspondence:

Sytle M. Antao
antao@ucalgary.ca

Specialty section:

This article was submitted to
Earth and Planetary Materials,
a section of the journal
Frontiers in Earth Science

Received: 11 July 2018

Accepted: 24 September 2018

Published: 22 October 2018

Citation:

Antao SM and Nicholls JW (2018)
Crystal Chemistry of Three Volcanic
K-rich Nepheline Samples From
Oldoinyo Lengai, Tanzania and Mount
Nyiragongo, Eastern Congo, Africa.
Front. Earth Sci. 6:155.
doi: 10.3389/feart.2018.00155

Natural nepheline (Nph) samples are intermediate members of solid solutions that extend from the pure Na end-member Na[AlSiO₄] to the pure K end-member K[AlSiO₄] (=kalsilite, Kls). We examined two volcanic nepheline (ideally, K₂Na₆[Al₈Si₈O₃₂] or Nph_{0.75}Kls_{0.25}) samples from Oldoinyo Lengai, Tanzania (samples 1 and 2) and a third sample 3 from Mount Nyiragongo, Eastern Congo. The crystal structure of these three samples was obtained using synchrotron high-resolution powder X-ray diffraction (HRPXRD) data and Rietveld structure refinements in space group *P*6₃. Satellite reflections were not observed in these samples. The EPMA composition of sample 1 is {K_{1.50}Na_{0.19}Ca_{0.07}□_{0.23}}_{Σ2}(Na)₆[Si_{8.35}Al_{7.48}Fe_{0.18}]_{Σ16.00}O₃₂. The A site contains 0.23 vacancies (□) with some Na and Ca atoms, whereas the B site is completely filled with only Na atoms. From the EPMA formula, K(sof) = 0.844 and Na(sof) = 1.0. The refinement unit-cell parameters are *a* = 10.00247(1), *c* = 8.38396(1) Å, *V* = 726.431(1) Å³; K(sof) = 0.779(2) and Na(sof) = 0.988(2). The composition of sample 2 is {K_{1.67}□_{0.33}}_{Σ2}(Na_{5.76}K_{0.174}Ca_{0.06})_{Σ6}[Si_{8.44}Al_{7.37}Fe_{0.20}]_{Σ16.01}O₃₂, so K(sof) = 0.835 and Na(sof) = 1.030. Sample 2 has *a* = 10.01769(2), *c* = 8.39586(2) Å, *V* = 729.678(1) Å³, K(sof) = 0.812(2), and Na(sof) = 0.995(2). Sample 3 is a three-phase (3a, 3b, 3c) intergrowth with an average formula of {K_{1.77}□_{0.23}}₂(Na_{4.30}K_{1.51}Ca_{0.19})_{Σ6}[Si_{8.13}Al_{7.76}Fe_{0.11}]_{Σ16.00}O₃₂, K(sof) = 0.887, and Na(sof) = 1.208. A large amount of K and Ca atoms occur in the B site. Based on the weight percentages and sofs of the three phases, the Rietveld refinement gives an average K(sof) = 0.859 and Na(sof) = 1.145. The average <*T*-O> distances indicate a high degree of Al-Si disorder in samples 1, 2, and phase 3b. These African samples extend natural nepheline solid solutions to about Nph_{0.55}Kls_{0.45}. The average <Na-O> distance increases linearly with Na(sof) and *V* across nepheline solid solutions because K atoms enter the Na site. K-rich nepheline seems to always contain vacancies in the A site.

Keywords: volcanic K-rich nepheline, kalsilite, crystal structure, Al-Si order, HRPXRD, intergrowths

INTRODUCTION

Nepheline (Nph), ideally $K_2Na_6[Al_8Si_8O_{32}]$, is an important rock-forming mineral that has wide occurrences in many silica-poor alkaline igneous rocks and related pegmatites. Nepheline is an intermediate member of a solid solution that extends from $Na[AlSiO_4]$ to $K[AlSiO_4]$ (=kalsilite, Kls). Although the nepheline-kalsilite series is commonly thought to involve only K-Na substitution, these solid solutions vary in Al-Si ratio and with Ca atoms or vacancies substituting for K and Na atoms. Nepheline often contains an excess amount of Si over Al atoms, which creates vacancies \square , because of the $\square Si^{4+} = (K,Na)^+ Al^{3+}$ and $\square Ca^{2+} = 2(K,Na)^+$ substitutions.

Both nepheline and kalsilite have a tridymite-type framework structure (e.g., Sahama, 1958; Capobianco and Carpenter, 1989; McConnell, 1991; Carpenter and Cellai, 1996; Xu and Veblen, 1996). Most common nepheline samples have a composition that is close to $K_2Na_6[Al_8Si_8O_{32}]$ with vacancies in the A site that contains K atoms, but nepheline from a few rare volcanic rocks are K-rich, so K atoms and vacancies occupy the A site and the remaining K atoms replace some of the Na atoms in the B site as indicated by the formula, $K_{3.11}Na_{4.20}Ca_{0.31}[Al_{7.64}Si_{8.01}O_{32}]$, which is analysis # 3, p. 478 in Deer et al. (1992). Such volcanic nepheline samples have unusual chemical compositions and large unit-cell parameters. The crystal structure of such an unusual nepheline is not known, but such samples extend the nepheline solid solutions considerably. For example, analysis #3 above is given as $Nph_{0.55}Kls_{0.45}$. The structure for a K-rich nepheline with a $Kls_{0.28}$ component was recently reported (Hamada et al., 2018). Because nepheline has a Na/K ratio of 3:1, the ideal formula corresponds to $(NaAlSiO_4)_{0.75}(KAlSiO_4)_{0.25}$ or $Nph_{0.75}Kls_{0.25}$. Nepheline from Oldoinyo Lengai, Tanzania contains $Kls_{0.25-0.27}$ (Dawson, 1998), whereas those from Mount Nyiragongo contains about $Kls_{0.45}$ (Sahama, 1962). The samples used in this study are from the above two localities. The crystal structure of such volcanic K-rich nepheline samples are unknown, so the aim of this study is to obtain the crystal structure of these samples. Such K-rich samples will also extend the natural nepheline solid solutions considerable, so the structural trends (bond distances and unit-cell parameters) are also analyzed in this study.

Diffraction data from some nepheline samples show satellite reflections with a wide range of intensity and sharpness (Sahama, 1958; McConnell, 1962, 1981, 1991; Sahama, 1962). The satellite reflections indicate that nepheline has a modulated structure with an incommensurate supercell. Various models have been proposed for the modulated structure of nepheline (McConnell, 1962; Parker and McConnell, 1971; Parker, 1972; McConnell, 1981; Merlino, 1984; McConnell, 1991; Hayward et al., 2000; Angel et al., 2008). Recently, a model for the incommensurately modulated structure of nepheline was presented in a superspace group by Friese et al. (2011). They indicated that all the atoms in the structure are displacively modulated with amplitudes below 0.1 Å.

The study examines two volcanic nepheline samples from Oldoinyo Lengai, Tanzania (samples 1 and 2) and a third sample 3 from Mount Nyiragongo, Eastern Congo (Zaire), Africa. The crystal structure of these three samples was obtained

using synchrotron high-resolution powder X-ray diffraction (HRPXRD) data and Rietveld structure refinements. The results indicate a high degree of Al-Si disorder in samples 1, 2, and phase 3b. The site-occupancy factors (*sofs*) for the A and B sites and the average $\langle A-O \rangle$ and $\langle B-O \rangle$ distances are rationalized in terms of the K, Na, and Ca atoms together with vacancies. These three samples extend nepheline solid solutions considerably to about $Nph_{0.55}Kls_{0.45}$, so variations in their unit-cell parameters are examined.

BACKGROUND INFORMATION

The structure of nepheline is a stuffed derivative of tridymite with half the Si replaced by Al atoms, and with Na and K as interstitial charge-balancing cations (Schiebold, 1930; Buerger et al., 1954; Hahn and Buerger, 1955). The structure of nepheline consists of four independent tetrahedral *T* (=Al or Si) sites per unit cell (Figure 1). The T_1 and T_2 sites occupy special positions on the three-fold axes, whereas the T_3 and T_4 sites occupy general positions. The apices of the T_1 and T_4 tetrahedra point to one

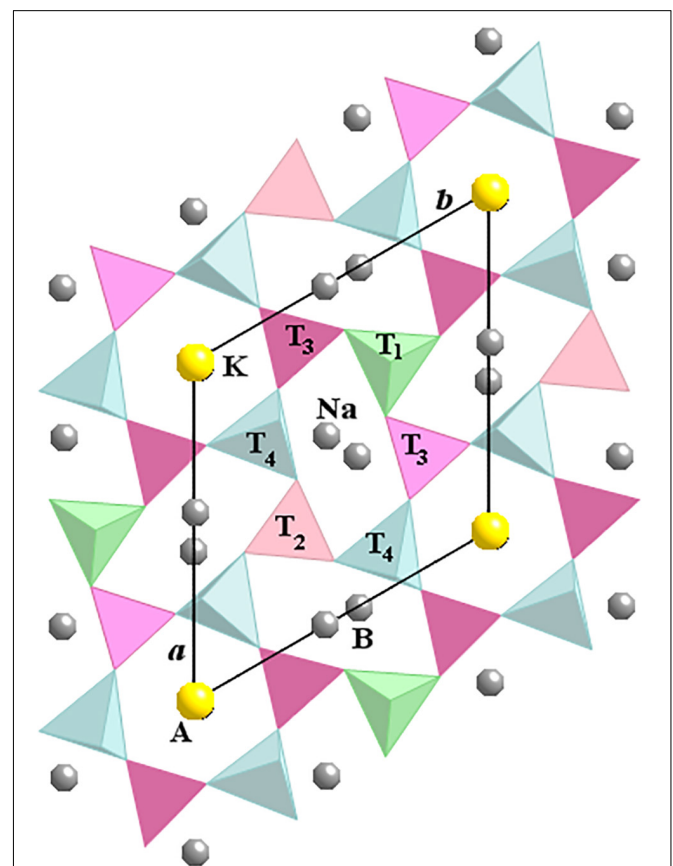
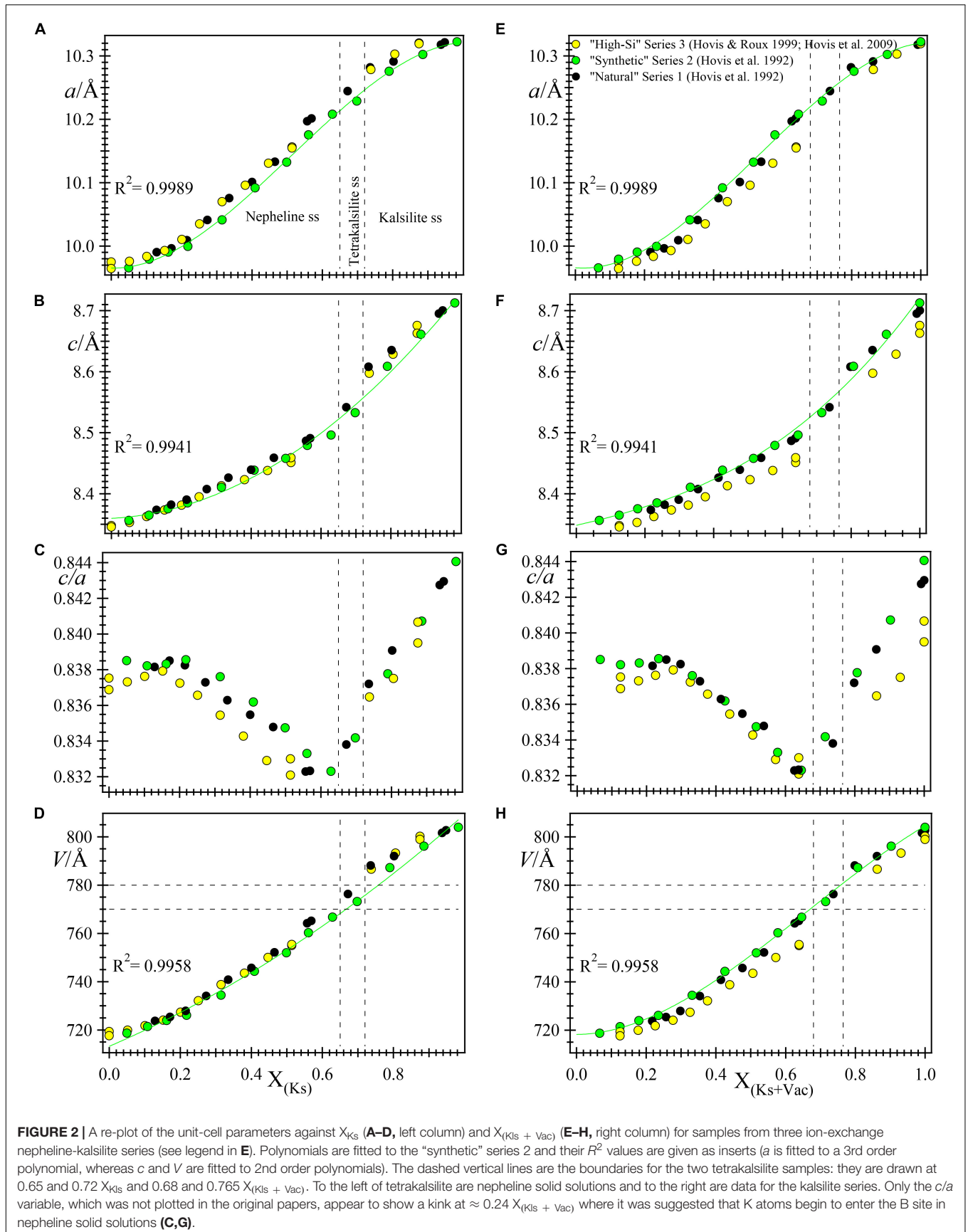


FIGURE 1 | Crystal structure of nepheline projected down the *c* axis. A is the hexagonal site that contains K atoms and vacancies, and B is the oval-shaped site that contains mostly Na atoms that may be substituted by Ca and K atoms. The T_2 and T_3 tetrahedra have apices pointing downwards, whereas T_1 and T_4 tetrahedra point upwards. The Al and Si atoms are highly ordered in the *T* sites for most nepheline samples.



direction along the *c* axis, whereas the T_2 and T_3 tetrahedra point in the opposite direction. The apical oxygen atom, O1, is slightly off the threefold axis toward one of the three neighboring Na atoms. The Na atoms occupy the six small oval-shaped B cavities, and the K atoms occupy two large hexagonal-shaped A cavities, which gives $\text{Na}_6\text{K}_2[\text{Al}_8\text{Si}_8\text{O}_{32}]$ as the ideal formula for nepheline. However, small amounts of Ca occur with Na atoms on the B site and vacancies occur with K atoms on the A site. Chemical analyses show that the Si *apfu* (atom per formula unit) is slightly more than the Al *apfu*.

The Al and Si atoms are ordered over the tetrahedral sites to a high degree in nepheline. The T_1 – T_2 (not T_3 – T_4) pair is bonded to the positionally disordered O1 atoms. In addition, the T_1 and T_2 tetrahedra are surrounded by only Na atoms, whereas the T_3 and T_4 tetrahedra are surrounded by both K and Na atoms.

The structure of nepheline from various geological settings was refined (Dollase, 1970; Foreman and Peacor, 1970; Dollase and Peacor, 1971; Simmons and Peacor, 1972; Dollase and Thomas, 1978; Gregorkiewitz, 1984; Hassan et al., 2003; Tait et al., 2003; Angel et al., 2008). The structure of a Ge-substituted analog of nepheline is also available (Hammond and Barbier, 1998). The crystal structures of nepheline, tetrakalsilite, and kalsilite were reviewed (Merlino, 1984). Al and Si atoms are ordered over the tetrahedral sites in nepheline. In general, the T_1 and T_4 sites are Al-rich, and the T_2 and T_3 sites are Si-rich (Foreman and Peacor, 1970; Dollase and Peacor, 1971; Simmons and Peacor, 1972). Structure refinements of five crystals with different thermal histories indicate a variable degree of Si–Al ordering depending on crystallization history (Dollase and Peacor, 1971). The Al and Si atoms in a nepheline from a low-temperature pegmatitic environment are highly ordered over all four tetrahedral sites with T_1 and T_4 containing most of the Al atoms and T_2 and T_3 most of the Si atoms (Foreman and Peacor, 1970). In contrast, the Al–Si distribution in a volcanic nepheline shows considerable disorder between T_1 and T_2 , but a high degree of order between T_3 and T_4 (Simmons and Peacor, 1972).

Variations in Unit-Cell Parameters for Synthetic Nepheline-Kalsilite Solid Solutions

Data for three ion-exchange series between nepheline (Nph; $\text{NaAlSi}_3\text{O}_8$) and kalsilite (Kls; KAlSi_3O_8) were reported in several related studies (e.g., Hovis et al., 1992, 2009; Hovis and Roux, 1999). The “natural” series 1 was made by K–Na ion exchange of a nepheline sample from Monte Somma with a composition $\text{Na}_{0.747}\text{Ca}_{0.036}\text{K}_{0.129}\square_{0.088}[\text{Al}_{0.948}\text{Si}_{1.052}\text{O}_4]$, which contains 5.2 mole % excess Si atoms and 3.6 mole % Ca atoms (Hovis et al., 1992). The amount of vacancies is, $\square_{0.088} = \text{Si}_{0.052} + \text{Ca}_{0.036}$. The “synthetic” series 2 was made by K–Na ion exchange of a sodic nepheline, $(\text{Na},\text{K})_{0.983}\square_{0.017}[\text{Al}_{0.983}\text{Si}_{1.017}\text{O}_4]$, hydrothermally synthesized from a gel and contain 1.7 mole % excess Si atoms and the same amount of vacancies (Hovis et al., 1992; Hovis and Roux, 1993). A “high-Si” series 3 contains 12.5 mole % excess Si atoms (Hovis and Roux, 1999; Hovis and Crelling, 2000; Hovis et al., 2009). Four chemical molecules or components were used to describe compositions in the nepheline–kalsilite

TABLE 1 | Chemical composition* for three nepheline samples from Africa.

	(1) ODL-2010-1	(2) ODL-2010-3	(3) NYIRA-1
SiO_2 (oxide Wt. %)	43.01 (46)	44.07 (83)	41.06 (35)
Al_2O_3	32.70 (27)	32.65 (34)	33.25 (13)
FeO	1.09 (16)	1.25 (14)	0.63 (03)
TiO_2	0.00 (00)	0.01 (01)	0.02 (01)
K_2O	6.07 (19)	7.55 (44)	12.98 (32)
Na_2O	16.46 (15)	15.53 (85)	11.21 (24)
CaO	0.34 (01)	0.31 (15)	0.90 (06)
Σ	99.66	101.36	100.02
<i>apfu</i> based on 32 O atoms			
Si	8.345	8.439	8.132
Al	7.477	7.368	7.761
Fe^{3+}	0.177	0.200	0.105
Ti	0.000	0.002	0.003
Σ	15.999	16.009	16.002
(Al + Si + Ti + Fe)			
K	1.502	1.844	3.279
Na	6.194	5.763	4.304
Ca	0.070	0.063	0.191
Σ (K + Na + Ca)	7.766	7.670	7.773
Vacancies in K or A site	0.234	0.330	0.226
EPMA: K(<i>sof</i>)	0.844	0.835	0.887
EPMA: Na(<i>sof</i>)	1.000	1.030	1.208
Refinement A site: K(<i>sof</i>)	0.779 (2)	0.812 (2)	0.860 (6)3a
			0.852 (5)3b
			0.869 (5)3c
Average (based on wt. % and <i>sofs</i>)			0.859
Refinement B site: Na(<i>sof</i>)	0.988 (2)	0.995 (2)	1.090 (5)3a
			1.162 (4)3b
			1.162 (5)3c
Average (based on wt. % and <i>sofs</i>)			1.145

*Average analyses from 12 points (*esds* are in brackets). Vacancies = $8 - \Sigma(\text{K} + \text{Na} + \text{Ca})$. Based on their EPMA formulae (below), the *sofs* of the B and A site are compared with those obtained from the structure refinement (last 10 lines):

(1) $\{\text{K}_{1.502}\text{Na}_{0.194}\text{Ca}_{0.070}\square_{0.234}\}_{\Sigma 2}(\text{Na})_6[\text{Si}_{8.345}\text{Al}_{7.477}\text{Fe}_{0.177}]\Sigma 15.999\text{O}_{32}$; K(*sof*) = 0.844, Na(*sof*) = 1.0.

(2) $\{\text{K}_{1.670}\square_{0.330}\}_{\Sigma 2}(\text{Na}_{5.763}\text{K}_{0.174}\text{Ca}_{0.063})\Sigma 6[\text{Si}_{8.439}\text{Al}_{7.368}\text{Fe}_{0.200}]\Sigma 16.009\text{O}_{32}$; K(*sof*) = 0.835, Na(*sof*) = 1.030.

(3) $\{\text{K}_{1.774}\square_{0.226}\}_{\Sigma 2}(\text{Na}_{4.304}\text{K}_{1.505}\text{Ca}_{0.191})\Sigma 6[\text{Si}_{8.132}\text{Al}_{7.761}\text{Fe}_{0.105}]\Sigma 16.002\text{O}_{32}$; K(*sof*) = 0.887, Na(*sof*) = 1.208.

series. These included Nph ($\text{NaAlSi}_3\text{O}_8$), Kls (KAlSi_3O_8), 2Qz ($\square\text{Si}_2\text{O}_4$), and 0.5An ($\square_{0.5}\text{Ca}_{0.5}\text{AlSi}_3\text{O}_8$), where X_{Nph} and X_{Kls} indicate the mole fraction of Nph, and Kls, respectively, \square are vacancies (Vac), where $X_{\text{Vac}} = X_{2\text{Qz}} + 0.5 X_{0.5\text{An}}$. Mole fractions (X) are related to the mole fractions of the chemical molecules: $X_{\text{Na}} = X_{\text{Nph}}$, $X_{\text{K}} = X_{\text{Kls}}$, $X_{\text{Ca}} = 0.5 X_{0.5\text{An}}$, and $X_{\text{Vac}} = X_{2\text{Qz}} + 0.5 X_{0.5\text{An}}$. Further details are given in the references above where they plot unit-cell parameters against compositions

TABLE 2 | Unit-cell and Rietveld refinement parameters for three nepheline samples.

Sample #	1 ODL-2010-1	2 ODL-2010-3	Phase 3a NYRA-1	Phase 3b NYRA-1	Phase 3c NYRA-1
wt. %	100	100	24.07(9)	45.80(9)	30.13(8)
2 θ range (°)	2–43	2–43	2–35		
N _{datapts}	41000	41000	33000		
N _{obs}	1427	1446	2490		
R _F ²	0.0534	0.0542	0.0361		
χ^2	1.171	1.752	1.626		
a (Å)	10.00247 (1)	10.01769 (2)	10.0565 (2)	10.0907 (1)	10.10183 (3)
c (Å)	8.38396 (1)	8.39586 (2)	8.4219 (2)	8.4357 (1)	8.44270 (3)
V (Å ³)	726.431 (1)	729.678 (2)	737.62 (3)	743.86 (1)	746.126 (4)
c/a	0.83819	0.83810	0.83746	0.83599	0.83576

Refinements were done in space group $P6_3$ using monochromatic $\lambda = 0.42465(2)$ Å. A smaller 2θ range was used for sample 3 because reflections beyond 33° 2θ were absent.

across the Nph-Kls series. Tetrakalsilite has the ideal formula $K_{0.625}Na_{0.375}[AlSiO_4]$. Ideal nepheline, $K_2Na_6[Al_8Si_8O_{16}]$ or $K_{0.25}Na_{0.75}[AlSiO_4]$, corresponds to Nph_{0.75}Kls_{0.25}.

In the original papers, the unit-cell data for the synthetic nepheline-kalsilite series were plotted against composition X_{Kls} and $X_{(Kls + Vac)}$, as shown in **Figure 2**. The c/a parameter versus composition was not plotted in the original papers (e.g., Hovis and Roux, 1999). The original data were represented by three linear segments that intersect where $X_{(Kls + Vac)}$ is about 0.24 and 0.74 (see Hovis et al., 1992). In **Figure 2**, except for the c/a versus compositional plots, all the other graphs are fitted in this study by polynomials to the “synthetic” series 2 data. These polynomials do not seem to contain significant changes in slopes at $X_{(Kls + Vac)} \approx 0.24$ or 0.74. However, the c/a ratio versus composition plots do seem to contain changes in slopes at the above points (**Figures 2C,G**). These changes in slopes or break in linear trend lines was also observed by Smith and Tuttle (1957) and Donnay et al. (1959), and presumably corresponds to the point at which K atoms begin to occupy the smaller Na or B site at $X_{(Kls + Vac)} \approx 0.24$ (Hovis et al., 1992). Whether this statement is true or not can be answered definitively with structure refinement data. It is clear from the plots (**Figures 2C,G**), change in slopes for unit-cell dimensions occur at the Nph–tetrakalsilite–Kls transitions near $X_{(Kls + Vac)} \approx 0.74$.

SAMPLE DESCRIPTION

We examined three samples of nepheline from two different volcanoes in Africa. Sample 1 (ODL-2010-1) and sample 2 (ODL-2010-3) are from the Oldoinyo Lengai Volcano, Tanzania. Sample 1 contains hexagonal shaped euhedral nepheline crystals together with aegirine and biotite. Sample 2 was collected from an ash fall that contains large (>0.05 mm diameter), well-developed, euhedral crystals of nepheline that occur with aegirine, augite, and olivine. Sample 3 (Nyra-1) is from the Mount Nyiragongo Volcano, Eastern Congo and contains nepheline with leucite and melilite. Another sample (ODL-2010-2) contains small (about 0.05 mm diameter) nepheline crystals that occur with aegirine and titanite. Because two

samples (ODL-2010-2 and ODL-2010-3) gave identical unit-cell parameters, sample (ODL-2010-2) was not investigated further.

EXPERIMENTAL

The three nepheline samples were analyzed using a JEOL JXA-8200 WD-ED electron-probe micro-analyzer (EPMA). The JEOL operating program on a Solaris platform was used for ZAF correction and data reduction. The wavelength-dispersive (WD) operating conditions were 15 kV accelerating voltage, 10 nA beam current, and 5 μ m beam diameter. $K\alpha$ radiation and the following standards were used: rutile (Ti), spinel (Al and Mg), hematite (Fe), wollastonite (Ca, Si), and feldspar (Na, K). The crystals appear to be homogeneous based on optical observations and microprobe analyses. **Table 1** contains the average chemical compositions from 12 spots together with their standard deviations.

Large single crystals of nepheline about 0.05 mm in diameter were hand-picked under a binocular microscope and finely ground in an agate mortar and pestle for synchrotron high-resolution powder X-ray diffraction (HRPXRD) experiments performed at beamline 11-BM, Advanced Photon Source, Argonne National Laboratory. Each sample was loaded into a Kapton capillary (0.8 mm internal diameter) and rotated during the experiment at a rate of 90 rotations per second. The data were collected to a maximum 2θ of about 43° with a step size of 0.001° and a step time of 0.1 s per step. The HRPXRD traces were collected with a unique multi-analyzer detection assembly consisting of twelve independent silicon (111) crystal analyzers and $LaCl_3$ scintillation detectors that reduce the angular range to be scanned and allow rapid acquisition of data. A silicon (NIST 640c) and alumina (NIST 676a) standard (ratio of 1/3 Si: 2/3 Al_2O_3 by weight) was used to calibrate the instrument and to refine the monochromatic wavelength [$\lambda = 0.42465(2)$ Å] used in the experiment. Additional details of the experimental set-up are given elsewhere (Antao et al., 2008; Lee et al., 2008; Wang et al., 2008).

TABLE 3 | Atom coordinates and U Parameters ($\times 100 \text{ \AA}^2$) for three nepheline samples.

Sample		1	2	3a	3b	3c
Al1	x	2/3	2/3	2/3	2/3	2/3
	y	1/3	1/3	1/3	1/3	1/3
	z	0.8101(6)	0.8073(5)	0.7990(24)	0.8115(8)	0.1870(19)
	U	0.996(9)	1.033(9)	1.022(11)	1.022(11)	1.022(11)
Si1	x	2/3	2/3	2/3	2/3	2/3
	y	1/3	1/3	1/3	1/3	1/3
	z	0.1964(5)	0.1940(5)	0.1888(22)	0.1964(8)	0.7991(18)
	U	0.996(9)	1.033(9)	1.022(11)	1.022(11)	1.022(11)
Si2	x	0.3314(2)	0.3330(3)	0.3362(10)	0.3301(6)	0.3311(6)
	y	0.0927(3)	0.0945(3)	0.0962(9)	0.0964(5)	0.0950(5)
	z	0.6882(1)	0.6872(3)	0.6797(15)	0.6906(6)	0.3042(10)
	U	0.996(9)	1.033(9)	1.022(11)	1.022(11)	1.022(11)
Al2	x	0.3364(2)	0.3351(4)	0.3318(10)	0.3350(6)	0.3376(5)
	y	0.0947(3)	0.0939(4)	0.0937(10)	0.0969(6)	0.1037(6)
	z	0.3140(1)	0.3132(4)	0.3067(15)	0.3158(6)	0.6791(11)
	U	0.996(9)	1.033(9)	1.022(11)	1.022(11)	1.022(11)
K	x	0	0	0	0	0
	y	0	0	0	0	0
	z	1.0009(7)	0.9966(7)	0.992(4)	0.9947(11)	0.9904(16)
	U	2.42(5)	2.15(5)	2.19(6)	2.19(6)	2.19(6)
	sof	0.779(2)	0.812(2)	0.860(6)	0.852(5)	0.869(5)
Na	x	0.4441(1)	0.4440(1)	0.44252(32)	0.44551(24)	0.44359(23)
	y	0.9979(1)	0.9971(1)	0.9958(4)	0.99692(30)	0.99370(28)
	z	0.9977(7)	0.9966(7)	0.9951(24)	0.9945(8)	0.9940(16)
	U	2.25(3)	2.29(4)	2.18(4)	2.18(4)	2.18(4)
	sof	0.988(2)	0.995(2)	1.090(5)	1.162(4)	1.162(5)
O1	x	0.7118(5)	0.7067(8)	0.7180(16)	0.6907(40)	0.7097(12)
	y	0.3439(12)	0.3387(16)	0.3475(34)	0.3221(49)	0.3470(30)
	z	0.9933(17)	0.9866(14)	0.9854(53)	0.9812(21)	0.9907(68)
	U	2.16(2)	2.17(3)	1.96(3)	1.96(3)	1.96(3)
O2	x	0.3167(2)	0.3160(2)	0.3197(6)	0.3161(5)	0.3173(4)
	y	0.0272(2)	0.0279(2)	0.0303(6)	0.0382(5)	0.0331(4)
	z	0.4987(9)	0.4980(9)	0.4962(34)	0.4994(14)	0.4901(23)
	U	2.16(2)	2.17(3)	1.96(3)	1.96(3)	1.96(3)
O3	x	0.5196(3)	0.5216(3)	0.4993(10)	0.5167(7)	0.5199(10)
	y	0.1681(3)	0.1713(4)	0.1645(11)	0.1754(7)	0.1684(10)
	z	0.7207(4)	0.7200(4)	0.7467(19)	0.7092(8)	0.7458(13)
	U	2.16(2)	2.17(3)	1.96(3)	1.96(3)	1.96(3)
O4	x	0.5137(3)	0.5129(4)	0.5325(9)	0.5137(8)	0.5078(9)
	y	0.1681(3)	0.1664(4)	0.1780(11)	0.1660(8)	0.1767(10)
	z	0.2371(4)	0.2355(4)	0.2466(17)	0.2364(9)	0.2566(13)
	U	2.16(2)	2.17(3)	1.96(3)	1.96(3)	1.96(3)
O5	x	0.2717(7)	0.2821(5)	0.2820(15)	0.2852(8)	0.2847(9)
	y	0.2247(8)	0.2303(6)	0.2332(15)	0.2370(9)	0.2306(10)
	z	0.3108(8)	0.3103(6)	0.3103(18)	0.3114(10)	0.3056(12)
	U	2.16(2)	2.17(3)	1.96(3)	1.96(3)	1.96(3)
O6	x	0.2772(7)	0.2682(5)	0.2647(15)	0.2591(8)	0.2611(10)
	y	0.2249(8)	0.2201(6)	0.2158(14)	0.2160(9)	0.2229(11)
	z	0.6873(8)	0.6881(7)	0.6867(20)	0.6923(11)	0.6907(11)
	U	2.16(2)	2.17(3)	1.96(3)	1.96(3)	1.96(3)

The occupancy for each of Al1, Si1 and O1 is 1/3. Other sites are fully occupied, except for the K and Na sites; their sofs were refined. The positions of the T sites in the 3c structure are interchanged when compared to the other structures because of the resulting $\langle T-O \rangle$ distances (Table 4). Al1 and Al2 sites may be referred to as T₁ and T₄ sites, respectively, and Si1 and Si2 sites as T₂ and T₃ sites, respectively.

TABLE 4 | Bond distances [Å] and angles [°] in three nepheline samples.

1, 2, 3a, 3b	1	2	3a	3b	3c	3c
Al1-O1 x 1	1.589(14)	1.551(11)	1.64(5)	1.466(18)	1.70(6)	Al1-O1 x 1
*Al1-O3 x 3	1.740(3)	1.710(4)	1.747(11)	1.778(7)	1.698(11)	†Al1-O4 x 3
<Al1-O> [4]	1.702	1.670	1.720	1.700	1.699	<Al1-O> [4]
Si1-O1 x 1	1.751(13)	1.782(11)	1.77(5)	1.842(17)	1.66(6)	Si1-O1 x 1
†Si1-O4 x 3	1.631(3)	1.648(3)	1.546(12)	1.656(7)	1.645(10)	*Si1-O3 x 3
<Si1-O> [4]	1.661	1.681	1.602	1.703	1.649	<Si1-O> [4]
Si2-O2	1.696(7)	1.698(7)	1.657(30)	1.698(11)	1.669(19)	Si2-O2
*Si2-O3	1.664(3)	1.668(4)	1.534(10)	1.645(8)	1.599(9)	†Si2-O4
Si2-O5	1.630(7)	1.663(6)	1.702(18)	1.636(10)	1.655(9)	Si2-O5
Si2-O6	1.661(6)	1.679(6)	1.682(16)	1.684(9)	1.566(9)	Si2-O6
<Si2-O> [4]	1.663	1.677	1.644	1.666	1.622	<Si2-O> [4]
Al2-O2	1.661(8)	1.659(8)	1.700(31)	1.635(12)	1.718(19)	Al2-O2
†Al2-O4	1.673(3)	1.683(4)	1.827(12)	1.712(9)	1.712(9)	*Al2-O3
Al2-O5	1.718(7)	1.697(6)	1.710(17)	1.721(10)	1.768(9)	Al2-O5
Al2-O6	1.701(7)	1.678(7)	1.663(17)	1.682(11)	1.729(10)	Al2-O6
<Al2-O> [4]	1.688	1.679	1.725	1.688	1.732	<Al2-O> [4]
Na-O1	2.551(4)	2.602(5)	2.533(13)	2.749(32)	2.635(10)	Na-O1
Na-O2	2.528(2)	2.540(2)	2.533(6)	2.601(5)	2.562(4)	Na-O2
Na-O3	2.752(5)	2.773(5)	2.571(20)	2.874(8)	2.596(14)	Na-O3
Na-O3	2.643(5)	2.658(5)	2.893(19)	2.666(9)	2.818(13)	Na-O3
Na-O4	2.496(5)	2.491(6)	2.647(20)	2.525(9)	2.749(13)	Na-O4
Na-O4	2.900(5)	2.895(5)	2.816(19)	2.879(9)	2.840(12)	Na-O4
Na-O5	2.547(7)	2.494(6)	2.472(18)	2.463(10)	2.520(11)	Na-O5
Na-O6	2.547(7)	2.609(6)	2.642(18)	2.715(9)	2.667(11)	Na-O6
<Na-O> [8]	2.621	2.633	2.638	2.684	2.673	<Na-O> [8]
<Na-O> [7]	2.630	2.637	2.653	2.675	2.679	<Na-O> [7]
K-O2 x 3	3.040(1)	3.035(2)	3.074(5)	3.016(4)	3.052(4)	K-O2 x3
K-O5 x 3	2.978(7)	3.039(6)	3.040(22)	3.084(10)	3.071(12)	K-O5 x3
K725-O6 x 3	2.992(7)	2.956(6)	2.950(26)	2.944(10)	2.992(13)	K-O6 x3
<K-O> [9]	3.003	3.010	3.021	3.015	3.038	<K-O> [9]
O1-O1	0.708(6)	0.652(7)	0.799(22)	0.546(21)	0.666(16)	O1-O1
Si1-O1-Al1	151.6(2)	153.8(3)	148.5(8)	157.7(8)	153.6(6)	Si1-O1-Al1
Si2-O2-Al2	138.3(1)	138.5(1)	138.7(3)	143.1(3)	138.4(2)	Si2-O2-Al2
Si2-O3-Al1	136.8(2)	137.5(3)	145.3(8)	137.4(5)	136.8(5)	Si1-O3-Al2
Si1-O4-Al2	141.0(3)	140.4(3)	139.4(7)	138.6(5)	149.2(5)	Si2-O4-Al1
Si2-O5-Al2	141.4(4)	142.4(4)	138.7(13)	142.3(7)	142.2(7)	Si2-O5-Al2
Si2-O6-Al2	141.0(4)	140.6(5)	143.0(14)	140.2(7)	143.6(7)	Si2-O6-Al2
<T-O-T> [6]	141.68	142.52	142.27	143.22	143.97	<T-O-T> [6]

*Bonded to O3 and †bonded to O4 because the T positions are interchanged (see Table 3). Average <Na-O>[7] distance does not include the Na-O1 distance.

RIETVELD STRUCTURE REFINEMENT

The crystal structure was modeled using the Rietveld method (Rietveld, 1969) that is incorporated in the GSAS program (Larson and Von Dreele, 2000) and using the EXPGUI interface (Toby, 2001). Initial structural parameters were taken from Hassan et al. (2003). The background was modeled with a Chebyshev polynomial (8 terms). In the GSAS program, the reflection-peak profiles were fitted using type-3 profile (pseudo-Voigt; Cagliotti et al., 1958; Thompson et al., 1987). The structure refinements were carried out by varying parameters in the following sequence: scale factor, background, cell, zero shift, profile, atom positions, isotropic displacement parameters, U ,

and site-occupancy factor ($sofs$) for the K and Na sites. Finally, all variables were refined simultaneously. We constrained similar atoms to have the same value for U . For example, all the O atoms in each sample were constrained to have the same U value and all the T atoms were constrained to have the same U value. No constraints were used for the atoms coordinates, but those coordinates that are constrained by symmetry were fixed. Based on synchrotron data that are similar to that used in this study, the structure of three pegmatitic nephelines were successfully refined using the procedure outlined above (Antao and Hassan, 2010b).

Sample 3 was modeled as a three-phase intergrowth of nepheline with slightly different structural parameters. Table 2 contains the cell parameters and other information regarding

data collection and refinement. **Table 3** contains the atom coordinates and isotropic displacement parameters. **Table 4** contains the bond distances and angles.

RESULTS AND DISCUSSION

Chemical Analyses

The chemical analyses for the three samples show that they not only cover the usual range for nepheline compositions, but they also show a considerable extension of natural nepheline solid solutions to about $\text{Nph}_{0.55}\text{Kls}_{0.45}$ (**Table 1**). The samples contain a small excess of Si over Al atoms, which is typical for nepheline, ideally $(\text{A})_2(\text{B})_6[\text{Al}_8\text{Si}_8]\text{O}_{32}$. The chemical formula for sample 1 is $\{\text{K}_{1.50}\text{Na}_{0.19}\text{Ca}_{0.07}\square_{0.23}\}_{\Sigma 2}(\text{Na})_6[\text{Si}_{8.35}\text{Al}_{7.48}\text{Fe}_{0.18}]\Sigma 16.00\text{O}_{32}$, which contains 0.23 vacancies, \square in the A site that contains K together with some Na and Ca atoms because the B site is filled with only Na atoms to the maximum amount possible, 6. Based on the above formula, the A site has $\text{K}(\text{sof}) = 0.844$ and the B site has $\text{Na}(\text{sof}) = 1.0$ compared to $\text{K}(\text{sof}) = 0.779(2)$ and $\text{Na}(\text{sof}) = 0.988(2)$ obtained from the refinement (see last 10 lines in **Table 1**). Because some small amounts of Na and Ca atoms occur in the A site, the average $\langle \text{K-O} \rangle$ distance is the shortest for the three samples (**Table 4**). A significant amount of Fe^{3+} replaces Al^{3+} cations in the T site. The sum of the tetrahedral T cations is at the ideal value of 16 (**Table 1**). Sample 1 is a Na-rich nepheline. In most common nepheline samples, the A site usually contains K atoms and vacancies, whereas the B site is filled with mostly Na atoms and a small amount of Ca atoms.

The chemical formula for sample 2 is $\{\text{K}_{1.67}\square_{0.33}\}_{\Sigma 2}(\text{Na}_{5.76}\text{K}_{0.17}\text{Ca}_{0.06})_{\Sigma 6}[\text{Si}_{8.44}\text{Al}_{7.37}\text{Fe}_{0.20}]\Sigma 16.01\text{O}_{32}$. The A site content is typical of nepheline samples having only K atoms and vacancies, as do samples from Bancroft, Ontario (Hassan et al., 2003; Antao and Hassan, 2010b). However, the B site contains a small amount of K atoms together with the usual Na and Ca atoms, so these volcanic nepheline compositions are unusual. The A site has $\text{K}(\text{sof}) = 0.835$ and the B site has $\text{Na}(\text{sof}) = 1.030$ compared to $\text{K}(\text{sof}) = 0.812(2)$ and $\text{Na}(\text{sof}) = 0.995(2)$ obtained from the refinement (**Table 1**). A serious error can be made by using the K atoms to fill the A site first, thus eliminating A site vacancies, and then placing any remaining K atoms in the B site. We avoided this error because we have *sofs* from Rietveld refinements to compare with the EPMA data (**Table 1**). The results clearly show that all vacancies must be placed in the A site and perhaps vacancies are necessary for the A site. Sample 2 is more K-rich than sample 1, so sample 2 has a larger unit-cell volume, *V*. A small number of K atoms enter the B site in sample 2, but there is no significant change for unit-cell or structural parameters between samples 1 and 2. The ion-exchange nepheline solid solutions indicate changes in slopes for unit-cell parameters where K atoms enter the B site (**Figure 2**).

The most interesting average chemical formula was obtained for sample 3, $\{\text{K}_{1.774}\square_{0.226}\}_{\Sigma 2}(\text{Na}_{4.304}\text{K}_{1.505}\text{Ca}_{0.191})_{\Sigma 6}[\text{Si}_{8.13}\text{Al}_{7.76}\text{Fe}_{0.11}]\Sigma 16.01\text{O}_{32}$, from Mount Nyiragongo Volcano, Eastern Congo, which contains a large amount of K atoms that is more than the ideal value of 2. Such an unusually K-rich nepheline is uncommon. In spite of the

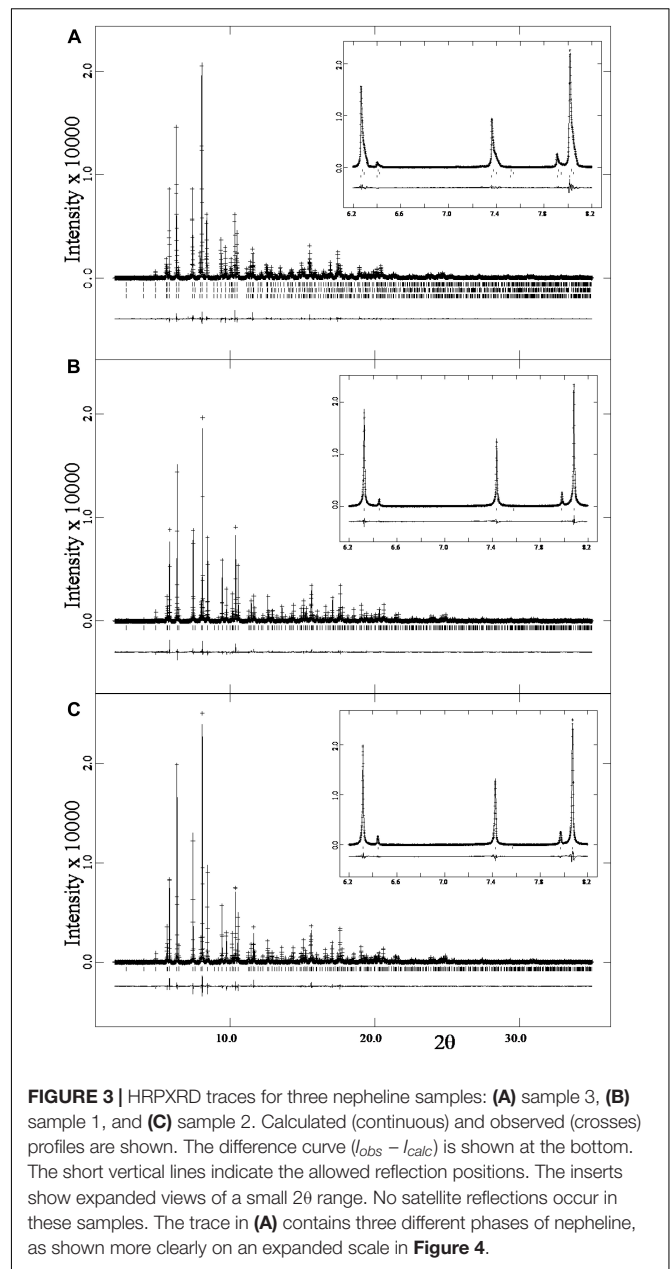


FIGURE 3 | HRPXRD traces for three nepheline samples: **(A)** sample 3, **(B)** sample 1, and **(C)** sample 2. Calculated (continuous) and observed (crosses) profiles are shown. The difference curve ($I_{\text{obs}} - I_{\text{calc}}$) is shown at the bottom. The short vertical lines indicate the allowed reflection positions. The inserts show expanded views of a small 2θ range. No satellite reflections occur in these samples. The trace in **(A)** contains three different phases of nepheline, as shown more clearly on an expanded scale in **Figure 4**.

large amounts of K atoms, the A site contains the usual amount of K atoms and vacancies. Some K atoms are placed in the B site together with Na and Ca atoms. Clearly, this sample is expected to have the largest unit-cell parameters among the three samples, which is indeed the case (**Table 2**). The A site has $\text{K}(\text{sof}) = 0.887$ and the B site has $\text{Na}(\text{sof}) = 1.208$ (**Table 1**).

Sample 3 contains a mixture of three phases, but only an average composition was obtained with EPMA. Based on the weight percentages of the three different phases (**Table 2**), the average $\text{K}(\text{sof}) = 0.859$ and average $\text{Na}(\text{sof}) = 1.145$ were obtained from the refinement (**Table 1**). $\text{Na}(\text{sof}) > 1$ is not unusual for nephelines because the B site contains Na, K, and Ca atoms. Other refinements of the nepheline structure also report $\text{Na}(\text{sof}) > 1$

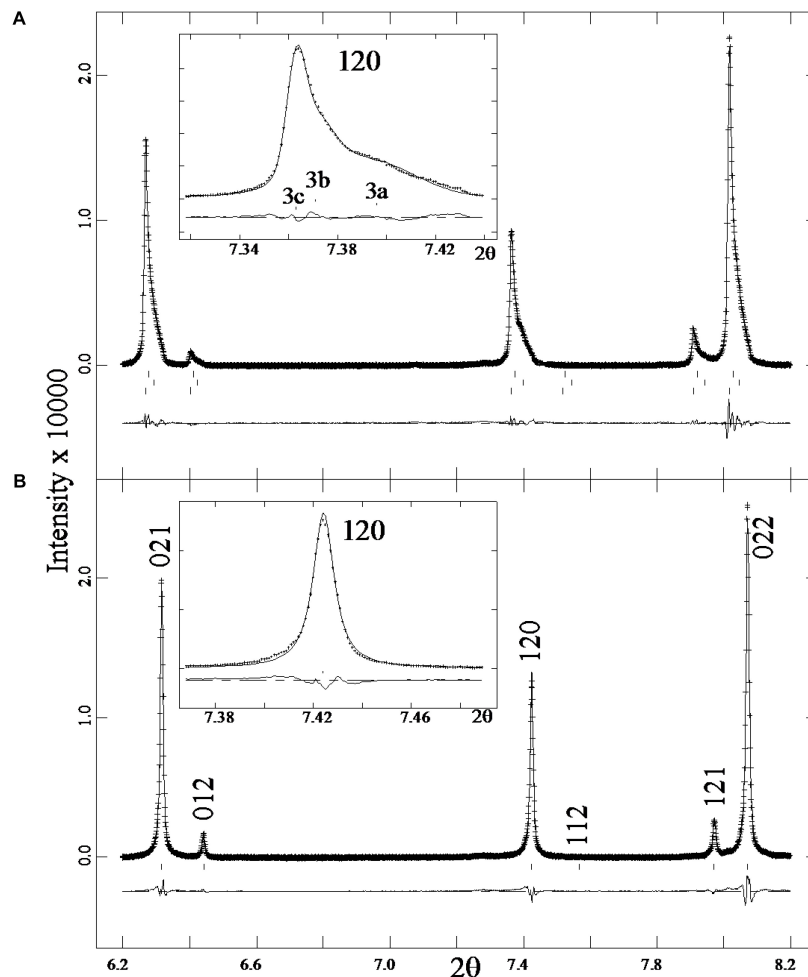


FIGURE 4 | Expanded views of a small 2θ range from the HRPXRD traces for **(A)** sample 3 and **(B)** sample 2. The diffraction peaks are symmetrical in **(B)** compared to the asymmetrical peaks in **(A)** that contain a three-phase intergrowth of nepheline. These features are shown more clearly in the inserts for the 120 peak. The three phases (3a, 3b, 3c) are labelled in **(A)** and they give rise to a “triplet” of splitting or “humps” in each diffraction peak.

(see **Figure 7A**). Moreover, it is not possible to constrain the refinement to the EPMA chemical composition because sample 3 contains a mixture of three phases. Vacancies and the presence of more than two different atoms on a site makes any chemical constraints unreliable for the nepheline structure. The structure refinement from Hamada et al. (2018) gives $0.968 \text{ Na} + 0.032 \text{ K}$ for the B site based on the assumption of full occupancy, whereas their EPMA gives $5.705 \text{ Na} + 0.198 \text{ K} + 0.031 \text{ Ca} + 0.034 \text{ Mg}$ with 0.032 vacancies. Both of these correspond to $\text{Na}(\text{sof}) = 1.023$.

In nepheline, the A site is not completely filled with K atoms. Vacancies are confined only to the A site. Some K atoms enter the B site, which is usually filled with mainly Na and minor amounts of Ca atoms. For assignments of atoms and vacancies to the A and B site to be correct, one must show from crystal structure refinements that the *sofs* and EPMA data match each other, which is the case in this study (**Table 1**).

Sahama (1962) also studied a nepheline sample from Nyiragongo, Congo (his sample no. 34) with a composition quite close to that obtained for

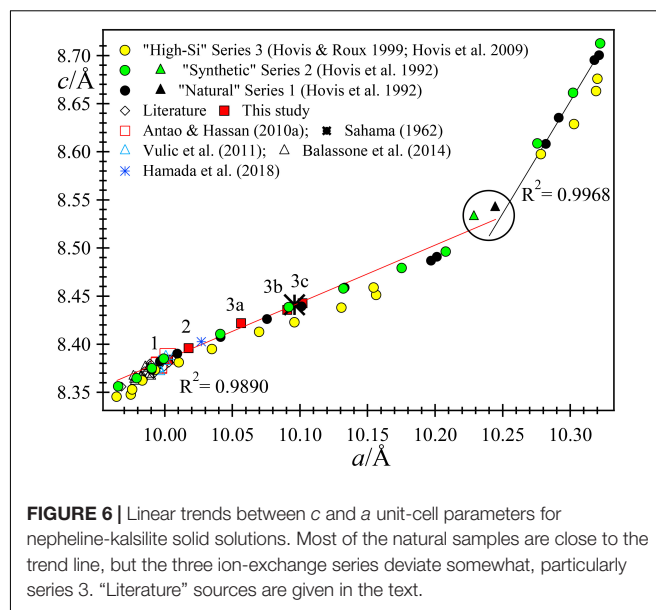
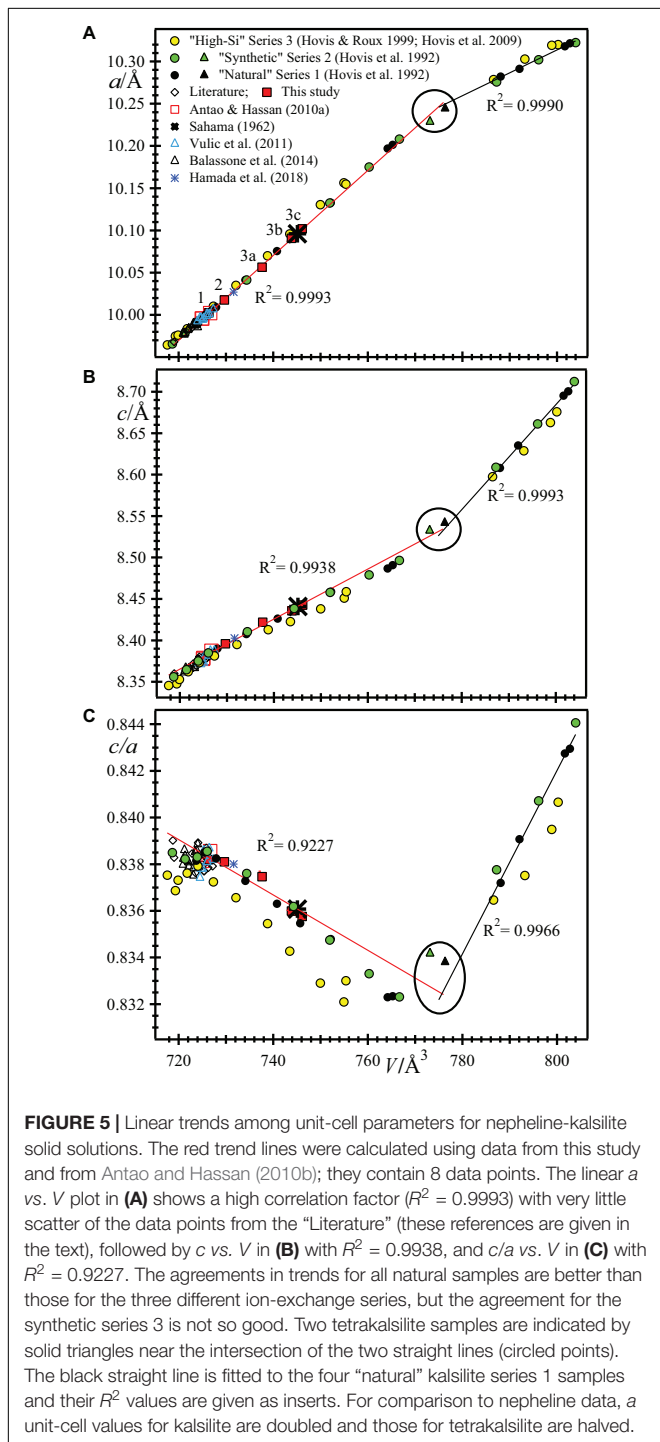
sample 3 in this study. A recalculation of the data from Sahama (1962) gives the formula $\{\text{K}_{1.58}\square_{0.42}\}_2 (\text{Na}_{4.23}\text{K}_{1.55}\text{Ca}_{0.23})_{\Sigma 6}[\text{Si}_{8.15}\text{Al}_{7.83}\text{Fe}_{0.04}]_{\Sigma 16.02}\text{O}_{32}$ with $a = 10.096$, $b = 8.441 \text{ \AA}$, and $V = 745.1 \text{ \AA}^3$ (see his pages 66 and 77) and these values are quite close to that obtained in this study (**Table 2**). The crystal structure of only one K-rich nepheline, $\{\text{K}_{1.74}\square_{0.26}\}_{\Sigma 2} (\text{Na}_{5.44}\text{K}_{0.51}\text{Ca}_{0.03}\text{Mg}_{0.02})_6[\text{Si}_{8.34}\text{Al}_{7.45}\text{Fe}_{0.16}]_{\Sigma 15.95}\text{O}_{32}$, from Japan was recently reported, but it is not as K-rich as our sample 3 (Hamada et al., 2018).

HRPXRD Traces and Satellite Reflections

The HRPXRD traces for the three nepheline samples used in this study contain no satellite reflections (**Figure 3**). Such reflections are easily observed in HRPXRD traces, and are common in nepheline that occurs in plutonic rocks and gneisses (see Antao and Hassan, 2010b). The trace shown in **Figure 3A** indicates a three-phase intergrowth of nepheline. The three phases are observed

by the asymmetry and splitting in the reflection peaks. The reflection peaks for samples 1 (**Figure 3B**) and 2 (**Figure 3C**) are more symmetrical than those shown for sample 3 (**Figure 3A**).

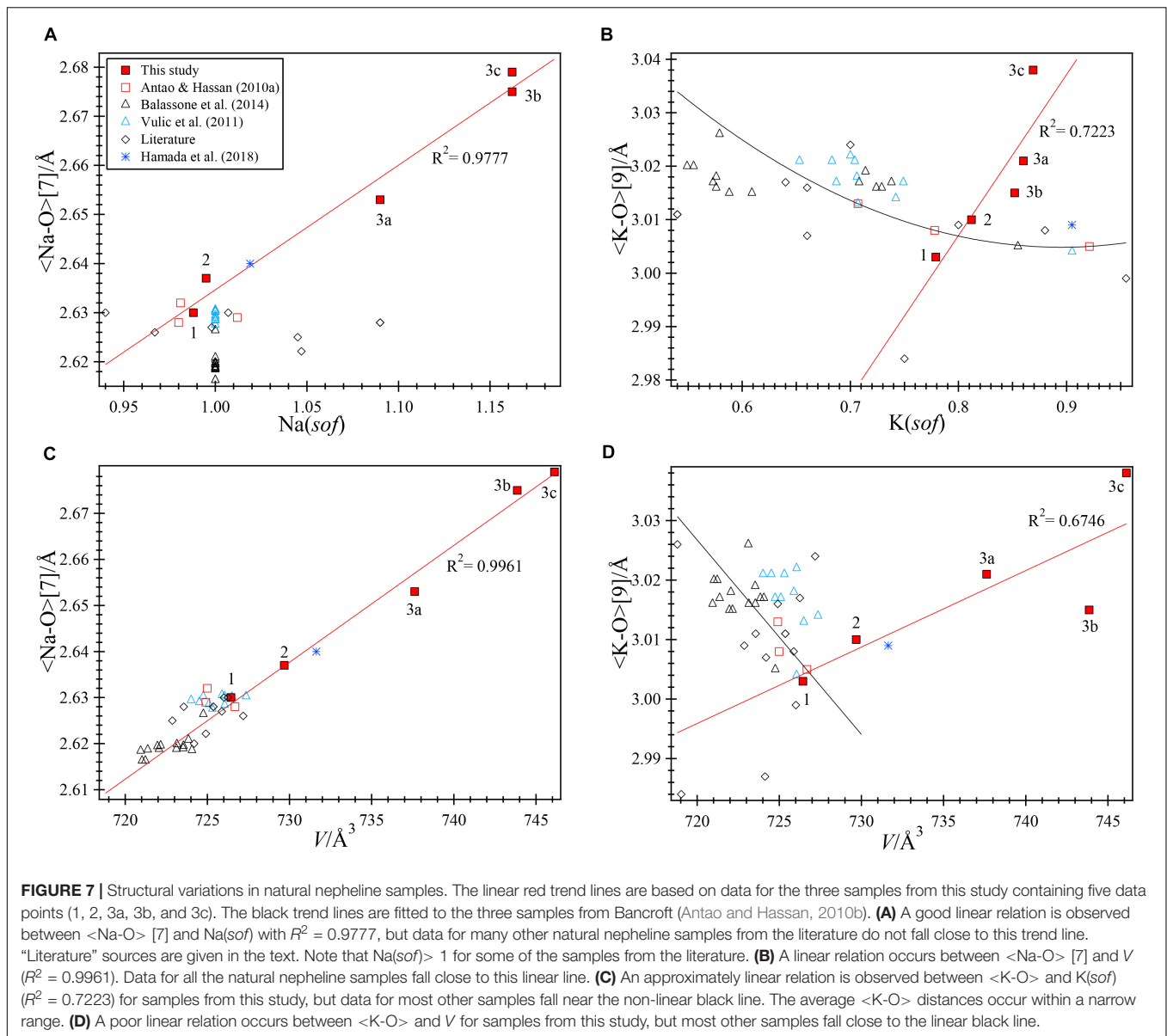
An expanded view of a small 2θ range shows a three-phase intergrowth for sample 3 (**Figure 4A**). The reflections peaks are symmetrical in **Figure 4B** compared to the asymmetrical



peaks in **Figure 4A** and the "triplet" splitting or "humps" indicate a three-phase intergrowth of nepheline. Hovis et al. (2009) showed a solvus in the nepheline-kalsilite system, so exsolution and intergrowths are expected for nepheline that cools slowly. The three phase intergrowth in sample 3 was not observed in back-scattered electron (BSE) images, which is not unusual because all three phases have quite similar structural features and compositions. In the case of genthelvite and garnet-group minerals, multi-phase intergrowths were observed by splitting of diffraction peaks, but only sometimes were the different phases observed in BSE images (Antao and Hassan, 2010a; Antao, 2013; Antao and Klincker, 2013; Antao et al., 2015a,b; Antao and Cruickshank, 2016).

Variations in Unit-Cell Parameters for Natural Nepheline Solid Solutions

Graphs of unit-cell data that are independent of compositions (**Figures 5, 6**) are compared to those that have compositions as variables (**Figure 2**) to see if the same general features are observed. The variations in unit-cell parameters for natural nepheline samples were not available because of the limited range in chemical composition. Our samples considerably extend the range of nepheline solid solutions. About one-half of the nepheline solid solution range is now covered by natural samples. Some excellent linear relations are observed for our natural samples. The linear trend lines pass through unit-cell parameters for other natural nepheline samples that vary within a very narrow range (**Figures 5, 6**). "Literature" data shown in **Figures 4–6** are taken from various studies (Dollase, 1970; Foreman and Peacor, 1970; Dollase and Peacor, 1971; Simmons and Peacor, 1972; Dollase and Thomas, 1978; Gregorkiewitz, 1984; Tait et al., 2003; Angel et al., 2008). Included in these figures are data from other studies as well, as indicated in their legends (Sahama, 1962; Antao and Hassan,



2010b; Vulic et al., 2011; Balassone et al., 2014; Hamada et al., 2018).

The variations of the a and V unit-cell parameter across the Nph-Kls series can be represented by two straight lines that intersect at tetrakalsilite. All the data points fall very close to the two trend lines, especially in **Figure 5A**, but less so in **Figure 5B**. The linear fits are quite good for natural nepheline samples and series 1 and 2 data, but not too good for series 3. The c/a versus V plot shows considerable scatter, especially for series 3 data (**Figure 5C**). Near the Kls side of the series, the variation is linear for series 1 and 2, but not for series 3. When the a and c parameters are plotted against each other, it appears that the variations are again linear, except for series 3 (**Figure 6**).

In the nepheline side of the series, the series 3 data appears to match two linear segments that meet at $V \approx 725 \text{ \AA}^3$,

which is not the case for the natural samples (**Figure 5C**). Is this break at $V \approx 725 \text{ \AA}^3$ real? Or are the unit-cell parameters for series 3 not measured accurately? The K atoms enters the B site between samples 1 ($V = 724.4 \text{ \AA}^3$) and 2 ($V = 729.7 \text{ \AA}^3$), where there are no significant changes in structural parameters, including unit-cell parameters. This substitution effect does not give rise to significant changes that were observed by others, e.g., **Figures 2C,G** (e.g., Hovis et al., 1992). It seems likely that all unit-cell parameters for both natural and synthetic samples should vary linearly among themselves (**Figures 5, 6**).

Sample 1 has small unit-cell parameters, which are similar to other Na-rich samples. Sample 3 has large unit-cell parameters, and sample 2 has intermediate values. Sample 3 contains an intergrowth of three phases that have different unit-cell

parameters (Figures 5, 6). It is interesting to note that the unit-cell data from Sahama (1962) match phases 3b and 3c quite well.

Structural Characteristics of the Three Nepheline Samples From Africa

The atom coordinates are similar for each sample (Table 3). After the $\langle T-O \rangle$ distances were computed, the Al1 and Si1 positions on one hand, and Al2 and Si2 positions on the other had to be interchanged in phase 3c because of the resulting $\langle T-O \rangle$ distances (see Table 3). The long and short average $\langle T-O \rangle$ distances correspond to Al-rich and Si-rich T sites, respectively (Table 4). These distances indicate some Al-Si order because the average $\langle Al-O \rangle$ distance is larger than the average $\langle Si-O \rangle$ distance. Average $\langle T-O \rangle$ distances of about 1.61 and 1.74 Å correspond to filled Si and Al sites, respectively, and indicate complete Si-Al order, whereas an average $\langle T-O \rangle$ distance of about 1.68 Å corresponds to complete Al-Si disorder (Hassan et al., 2004, 2006). A high degree of disorder is observed in samples 1, 2, and phase 3b because their average $\langle T-O \rangle$ distances are close to 1.68 Å (Table 4). Phases 3a and 3c contain some Al-Si order.

The O1 position may not be located accurately because of O1 disorder, so the Na-O1 distance is not included in the average $\langle Na-O \rangle$ [7] distance. The average $\langle K-O \rangle$ [9] and $\langle Na-O \rangle$ [7] distances can be rationalized with the atoms occupying the A and B sites, their *sofs*, and their effects on the unit-cell volume, V . Two excellent linear relations are observed for the samples used in this study (Figures 7A,B). The average $\langle Na-O \rangle$ [7] distances vary linearly with $Na(sof)$ and with V . The average $\langle Na-O \rangle$ [7] distances and V are large for phases 3b and 3c because they contain K atoms in the B site. Increase in $Na(sof)$ causes the average $\langle Na-O \rangle$ [7] distance and V to increase because of increasing amounts of K atoms entering the B site. Phases 3b and 3c have the highest $Na(sof)$ and have the largest average $\langle Na-O \rangle$ distance and V (Figures 7A,B). Although phases 3b and 3c have the largest but same $Na(sof)$, the $\langle Na-O \rangle$ [7] distance in phase 3b is slightly shorter than that for phase 3c probably because phase 3b contains more Ca atoms in the B site. Phase 3a must contain some K atoms in the B site because $\langle Na-O \rangle$ is larger than that for samples 1 and 2. The B site in sample 1 is filled with the maximum amount of Na atoms (=6), which is confirmed by the structure refinement that gives $Na(sof) = 0.988(2)$, average $\langle Na-O \rangle$ [7] = 2.630 Å, and $V = 726.431(1)$ Å³. These are considered as base point values, so if $Na(sof)$, $\langle Na-O \rangle$, and V increase from these base values, only K atoms could enter the B site, and not smaller Ca²⁺ cations or vacancies. If average $\langle Na-O \rangle$ and V decrease from the base values, then some Ca atoms must enter the B site. If Ca atoms occur in the B site, the $Na(sof)$ will increase, but not the average $\langle Na-O \rangle$ distance. It is important to note that K atoms begin to enter the B site between samples 1 and 2, where no significant structural changes are observed.

The average $\langle Na-O \rangle$ distances of all the samples studied by Balassone et al. (2014) are very similar to each other, which is consistent with full occupancy of the B site with Na atoms, so

their $Na(sof)$ was fixed at 1 (Figure 7A). Similar results were obtained for another set of samples (Vuliæ et al., 2011).

Vacancies and K atoms are present in the A site, but $K(sof)$ influence on the V and $\langle K-O \rangle$ [9] are not strongly correlated (Figures 7C,D). The $K(sof)$ vary from about 0.78 to 0.87 in our three samples and it varies approximately linearly with $\langle K-O \rangle$ (Figure 7C) and this distance increases approximately linearly with V (Figure 7D). Although $K(sof)$ is changing, the average $\langle K-O \rangle$ distance changes within a narrow limit (about 0.06 Å) and most samples have values between 3 and 3.03 Å. Phases 3b and 3c contain the most K atoms in the B site and have the largest V . In terms of average $\langle K-O \rangle$ distance and V , nepheline samples may be placed in two groups (Figure 7D). One group contains K atoms in the B site (samples 2, 3, and that from Hamada et al., 2018) and the other group contains no K atoms in the B site and includes most of the other samples that fall close to the linear black line.

CONCLUSION

Natural nepheline has a small excess of Si over Al atoms and vacancies occur in the A site. The Na/K ratio deviates from 3:1 in the ideal formula, $K_2Na_6[Al_8Si_8O_{16}]$. Our volcanic nepheline samples contain a high degree of Al-Si disorder in samples 1, 2, and 3b. Vacancies occur in the A site because of the $(Na,K)^+Al^{3+} = \square Si^{4+}$ substitution (this may also be written as $(Na,K)Al\square_{-1}Si_{-1}$). If the B site is filled, Na and Ca substitute for K atoms in the A site, as in sample 1. The $2(K,Na)^+ = \square Ca^{2+}$ substitution (or $2(K,Na)\square_{-1}Ca_{-1}$) also introduces vacancies in the A site. The above substitutions give rise to Na-rich nepheline solid solutions. The substitution of K for Na atoms in the B site gives rise to K-rich nepheline solid solutions, as in samples 2 and 3. The plagioclase feldspar substitution $[CaAlNa_{-1}Si_{-1}]$ plays an insignificant role in the nepheline-kalsilite series. There is no significant change in unit-cell or structural parameters when K atoms enter the B site. The average $\langle Na-O \rangle$ [7] distance increases linearly with $Na(sof)$ and V across nepheline solid solutions.

AUTHOR CONTRIBUTIONS

SA selected the crystals and did the structure refinements. JN collected the samples and obtained the chemical compositions.

ACKNOWLEDGMENTS

We thank the two reviewers and the Editor, F. Brunet, for useful comments that helped to improve this manuscript. Robert Marr is thanked for his help with the EPMA analysis. The HRPXRD data were collected at beamline 11-BM, Advanced Photon Source, Argonne National Laboratory. Use of the Advanced Photon Source was supported by the United States Department of Energy, Office of Science, Office of Basic Energy Sciences, under Contract No. DE-AC02-06CH11357. This work was supported with a NSERC Discovery Grant to SA.

REFERENCES

- Angel, R. J., Gatta, G. D., Boffa Ballaran, T., and Carpenter, M. A. (2008). The mechanism of coupling in the modulated structure of nepheline. *Can. Mineral.* 46, 1465–1476. doi: 10.3749/canmin.46.6.1465
- Antao, S. M. (2013). Three cubic phases intergrown in a birefringent andradite-grossular garnet and their implications. *Phys. Chem. Miner.* 40, 705–716. doi: 10.1007/s00269-013-0606-4
- Antao, S. M., and Cruickshank, L. A. (2016). Two cubic phases in kimzeyite garnet from the type locality Magnet Cove, Arkansas. *Acta Crystallogr.* B72, 846–854. doi: 10.1107/S2052520616014700
- Antao, S. M., and Hassan, I. (2010a). A two-phase intergrowth of genthelvite from Mont Saint-Hilaire, Quebec. *Can. Mineral.* 48, 1217–1223. doi: 10.3749/canmin.48.5.1217
- Antao, S. M., and Hassan, I. (2010b). Nepheline: structure of three samples from the bancroft area, Ontario, obtained using synchrotron high-resolution powder x-ray diffraction. *Can. Mineral.* 48, 69–80. doi: 10.3749/canmin.48.1.69
- Antao, S. M., Hassan, I., Wang, J., Lee, P. L., and Toby, B. H. (2008). State-of-the-art high-resolution powder x-ray diffraction (HRPXRD) illustrated with rietveld structure refinement of quartz, sodalite, tremolite, and meionite. *Can. Mineral.* 46, 1501–1509. doi: 10.3749/canmin.46.5.1501
- Antao, S. M., and Klinck, A. M. (2013). Origin of birefringence in andradite from Arizona, Madagascar, and Iran. *Phys. Chem. Miner.* 40, 575–586. doi: 10.1007/s00269-013-0594-4
- Antao, S. M., Zaman, M., Gontijo, V. L., Camargo, E. S., and Marr, R. A. (2015a). Optical anisotropy, zoning, and coexistence of two cubic phases in andradites from Quebec and New York. *Contrib. Mineral. Petrol.* 169:10. doi: 10.1007/s00410-015-1104-0
- Antao, S. M., Mohib, S., Zaman, M., and Marr, R. A. (2015b). Ti-rich andradites: chemistry, structure, multi-phases, optical anisotropy, and oscillatory zoning. *Can. Miner.* 53, 133–158. doi: 10.3749/canmin.140.0042
- Balassone, G., Kahlenberg, V., Altomare, A., Mormone, A., Rizzi, R., Saviano, M., et al. (2014). Nephelines from the Somma-Vesuvius volcanic complex (southern Italy): crystal-chemical, structural and genetic investigations. *Mineral. Petrol.* 108, 71–90. doi: 10.1007/s00710-013-0290-6
- Buerger, M. J., Klein, G. E., and Donnay, G. (1954). Determination of the crystal structure of nepheline. *Am. Mineral.* 39, 805–818.
- Cagliotti, G., Paoletti, A., and Ricci, F. P. (1958). Choice of collimators for a crystal spectrometer for neutron diffraction. *Nucl. Instrum.* 3, 223–228. doi: 10.1016/0369-643X(58)90029-X
- Capobianco, C., and Carpenter, M. (1989). Thermally induced changes in kalsilite (KAlSiO₄). *Am. Mineral.* 74, 797–811.
- Carpenter, M., and Cellai, D. (1996). Microstructures and high-temperature phase transitions in kalsilite. *Am. Mineral.* 81, 561–584. doi: 10.2138/am-1996-5-604
- Dawson, J. B. (1998). Peralkaline nepheline-natrocarbonate relationships at Oldoinyo Lengai, Tanzania. *J. Petrol.* 39, 2077–2094. doi: 10.1093/ptro/39.11-12.2077
- Deer, W. A., Howie, R. A., and Zussman, J. (1992). *An Introduction to the Rock-Forming Minerals*, 2nd Edn. New York, NY: John Wiley.
- Dollase, W. A. (1970). Least-squares refinement of the structure of a plutonic nepheline. *Z. Kristallogr.* 132, 27–44. doi: 10.1524/zkri.1970.132.1-6.27
- Dollase, W. A., and Peacor, D. R. (1971). Si-Al ordering in nephelines. *Contrib. Mineral. Petrol.* 30, 129–134. doi: 10.1007/BF00372253
- Dollase, W. A., and Thomas, W. M. (1978). The crystal chemistry of silica-rich, alkali-deficient nepheline. *Contrib. Mineral. Petrol.* 66, 311–318. doi: 10.1007/BF00373415
- Donnay, G., Schairer, J. F., and Donnay, J. D. H. (1959). Nepheline solid solutions. *Mineral. Mag.* 32, 93–109.
- Foreman, N., and Peacor, D. R. (1970). Refinement of the nepheline structure at several temperatures. *Z. Kristallogr.* 132, 45–70. doi: 10.1524/zkri.1970.132.1-6.45
- Friese, K., Grzechnik, A., Petöiaek, V., Schönleber, A., van Smaalen, S., and Morgenroth, W. (2011). Modulated structure of nepheline. *Acta Crystallogr.* B67, 18–29. doi: 10.1107/S0108768110050822
- Gregorkiewicz, M. (1984). Crystal structure and Al/Si-ordering of a synthetic nepheline. *Bull. Minéral.* 107, 499–509.
- Hahn, T., and Buerger, M. J. (1955). The detailed structure of nepheline, KNa₃Al₄Si₄O₁₆. *Z. Kristallogr.* 106, 308–338.
- Hamada, M., Akasaka, M., and Ohfuji, H. (2018). Crystal chemistry of K-rich nepheline in nephelinite from Hamada, Shimane Prefecture, Japan. *Mineral. Mag.* doi: 10.1180/mgm.2018.133
- Hammond, R. P., and Barbier, J. (1998). Monoclinic and hexagonal nepheline structures of (Na₃/4K_{1/4})AlGeO₄. *Acta Crystallogr.* B54, 211–220. doi: 10.1107/S0108768197013177
- Hassan, I., Antao, S. M., and Hersi, A. A. (2003). Single-crystal XRD, TEM, and thermal studies of the satellite reflections in nepheline. *Can. Mineral.* 41, 759–783. doi: 10.2113/gscanmin.41.3.759
- Hassan, I., Antao, S. M., and Parise, J. B. (2004). Sodalite: high temperature structures obtained from synchrotron radiation and rietveld refinements. *Am. Mineral.* 89, 359–364. doi: 10.2138/am-2004-2-315
- Hassan, I., Antao, S. M., and Parise, J. B. (2006). Cancrinite: crystal structure, phase transitions, and dehydration behavior with temperature. *Am. Mineral.* 91, 1117–1124. doi: 10.2138/am.2006.2013
- Hayward, S. A., Pryde, A. K. A., De Dombal, R. F., Carpenter, M. A., and Dove, M. T. (2000). Rigid unit modes in disordered nepheline: a study of a displacive incommensurate phase transition. *Phys. Chem. Miner.* 27, 285–290. doi: 10.1007/s002690050257
- Hovis, G. L., and Crelling, J. A. (2000). The effects of excess silicon on immiscibility in the nepheline-kalsilite system. *Am. J. Sci.* 300, 238–249. doi: 10.2475/ajs.300.3.238
- Hovis, G. L., Mott, A., and Roux, J. (2009). Thermodynamic, phase equilibrium, and crystal chemical behaviour in the nepheline-kalsilite system. *Am. J. Sci.* 309, 397–419. doi: 10.2475/05.2009.02
- Hovis, G. L., and Roux, J. (1993). Thermodynamic mixing properties of nepheline-kalsilite crystalline, solutions. *Am. J. Sci.* 293, 1108–1127. doi: 10.2475/ajs.293.10.1108
- Hovis, G. L., and Roux, J. (1999). Thermodynamics of excess silicon in nepheline and kalsilite crystalline solutions. *Eur. J. Mineral.* 11, 815–827. doi: 10.1127/ejm/11/5/0815
- Hovis, G. L., Spearing, D. R., Stebbins, J. F., Roux, J., and Clare, A. (1992). X-ray powder diffraction and ²³Na, ²⁷Al, and ²⁹Si MAS-NMR investigation of nepheline-kalsilite crystalline solutions. *Am. Mineral.* 77, 19–29.
- Larson, A. C., and Von Dreele, R. B. (2000). *General Structure Analysis System (GSAS)*. Los Alamos, NM: Los Alamos National Laboratory Report, LAUR, 86–748.
- Lee, P. L., Shu, D., Ramanathan, M., Preissner, C., Wang, J., Beno, M. A., et al. (2008). A twelve-analyzer detector system for high-resolution powder diffraction. *J. Synchrotron. Radiat.* 15, 427–432. doi: 10.1107/S0909049508018438
- McConnell, J. D. C. (1962). Electron-diffraction study of subsidiary maxima of scattered intensity in nepheline. *Mineral. Mag.* 33, 114–125.
- McConnell, J. D. C. (1981). Time-temperature study of the intensity of satellite reflections in nepheline. *Am. Mineral.* 66, 990–996.
- McConnell, J. D. C. (1991). Incommensurate structures. *Philos. Trans. R. Soc. Lond.* A334, 425–437. doi: 10.1098/rsta.1991.0023
- Merlino, S. (1984). “Feldspathoids: their average and real structures,” in *Feldspars and Feldspathoids, Nato ASI Series C*, ed. W. L. Brown (Dordrecht: D. Reidel Publishing Company), 137, 435–470.
- Parker, J. M. (1972). The domain structure of nepheline. *Z. Kristallogr.* 136, 255–272. doi: 10.1524/zkri.1972.136.3-4.255
- Parker, J. M., and McConnell, J. D. C. (1971). Transformation behaviour in the mineral nepheline. *Nature* 234, 178–179.
- Rietveld, H. M. (1969). A profile refinement method for nuclear and magnetic structures. *J. Appl. Crystallogr.* 2, 65–71. doi: 10.1107/S0021889869006558
- Sahama, T. G. (1958). A complex form of natural nepheline from Iivaara, Finland. *Am. Mineral.* 43, 165–166.
- Sahama, T. H. G. (1962). Order-disorder in natural nepheline solid solutions. *J. Petrol.* 3, 65–81. doi: 10.1093/petrology/3.1.65
- Schiebold, E. (1930). Zur struktur von nepheline and analcim. *Naturwiss* 1S, 705–706. doi: 10.1007/BF01513361

- Simmons, W. B., and Peacor, D. R. (1972). Refinement of the crystal structure of a volcanic nepheline. *Am. Mineral.* 57, 1711–1719.
- Smith, J. V., and Tuttle, O. F. (1957). The nepheline-kalsilite system: i. x-ray data for the crystalline phases. *Am. J. Sci.* 255, 282–305. doi: 10.2475/ajs.255.4.282
- Tait, K. T., Sokolova, E., Hawthorne, F. C., and Khomyakov, A. P. (2003). The crystal chemistry of nepheline. *Can. Mineral.* 41, 61–70. doi: 10.2113/gscanmin.41.1.61
- Thompson, P., Cox, D. E., and Hastings, J. B. (1987). Rietveld refinement of Debye-Scherrer synchrotron x-ray data from alumina. *J. Appl. Crystallogr.* 20, 79–83. doi: 10.1107/S0021889887087090
- Toby, B. H. (2001). EXPGUI, a graphical user interface for GSAS. *J. Appl. Crystallogr.* 34, 210–213. doi: 10.1107/S0021889801002242
- Vulić, R., Baliać-Zunić, T., Belmonte, L. J., and Kahlenberg, V. (2011). Crystal chemistry of nephelines from ijolites and nepheline-rich pegmatites: influence of composition and genesis on the crystal structure investigated by x-ray diffraction. *Mineral. Petrol.* 101, 185–194. doi: 10.1007/s00710-010-0143-5
- Wang, J., Toby, B. H., Lee, P. L., Ribaud, L., Antao, S. M., Kurtz, C., et al. (2008). A dedicated powder diffraction beamline at the advanced photon source: commissioning and early operational results. *Rev. Sci. Instrum.* 79:085105. doi: 10.1063/1.2969260
- Xu, H., and Veblen, D. R. (1996). Superstructures and domain structures in natural and synthetic kalsilite. *Am. Mineral.* 81, 1360–1370. doi: 10.2138/am-1996-11-1208

Conflict of Interest Statement: The authors declare that the research was conducted in the absence of any commercial or financial relationships that could be construed as a potential conflict of interest.

Copyright © 2018 Antao and Nicholls. This is an open-access article distributed under the terms of the Creative Commons Attribution License (CC BY). The use, distribution or reproduction in other forums is permitted, provided the original author(s) and the copyright owner(s) are credited and that the original publication in this journal is cited, in accordance with accepted academic practice. No use, distribution or reproduction is permitted which does not comply with these terms.